ABSTRACT

Title of Thesis: THERMOREVERSIBLE TRANSITIONS BETWEEN SELF-ASSEMBLED NANOSTRUCTURES IN AQUEOUS SOLUTION

Degree Candidate: TANNER S. DAVIES

Degree and Year: MASTER OF SCIENCE, 2005

Directed by: PROF. SRINIVASA R. RAGHAVAN,
DEPARTMENT OF CHEMICAL ENGINEERING

We study an unusual transition between two different types of self-assembled structures in aqueous solutions. Mixtures of a cationic surfactant, CTAB and the organic compound, 5-methyl salicylic acid (5mS) spontaneously self-assemble into unilamellar vesicles at room temperature. Upon heating, these vesicles undergo a thermoreversible transition to "wormlike" micelles, i.e., long, flexible micellar chains. This phase transition results in a *1000-fold increase in the solution viscosity* with increasing temperature. Small-angle neutron scattering (SANS) measurements show that the phase transition from vesicles to micelles is a continuous one, with the vesicles and micelles co-existing over a range of temperatures. The tunable vesicle-to-micelle transition and the concomitant viscosity increase upon heating may have utility in a range of areas including microfluidics, drug delivery, and enhanced oil recovery.

THERMOREVERSIBLE TRANSITIONS BETWEEN SELF-ASSEMBLED NANOSTRUCTURES IN AQUEOUS SOLUTION

Tanner S. Davies

Thesis submitted to the Faculty of the Graduate School of the
University of Maryland, College Park, in partial fulfillment
of the requirements for the degree of
Master of Science
2005

Advisory Committee:
Prof. Srinivasa R. Raghavan, Dept. of Chemical Engineering, Chair
Prof. Timothy A. Barbari, Dept. of Chemical Engineering
Prof. Sheryl H. Ehrman, Dept. of Chemical Engineering

Dedication

I would like to dedicate this thesis to all the people in my life who stood by me as I worked on this endeavor. Without their support and encouragement this would not have been possible.

Foremost I would like to thank my mother, Karen Davies for her unwavering support for me through all the challenges I've encountered in pursuit of my goals. For my entire life she has encouraged me to always better myself and to challenge myself continually.

I would also like to thank my extended family; John, Cindy, Cassandra, and Brady Collier, Gene, Kendra, Niko and Kayla Johnson, Ha Le, and Christopher O'Connor. Numerous times I faltered, and they were always there to help me back up. I appreciate all the conversations we've had when I doubted myself.

Acknowledgements

I would also like to acknowledge several people who provided me with the foundation to complete this work. First I would like to thank my advisor Dr. Srinivasa Raghavan for his support, encouragement and guidance during my matriculation here at the University of Maryland, College Park. I would like to thank Dr. Sheryl Ehrman and Dr. Timothy Barbari for serving on my committee. Jae-Ho Lee, Bani Cipriano, Shih-Huang Tung and Gokul Kalur need to be thanked for the many discussions on a variety topics regarding this work, and for always being there with a helping hand and a smile. Also I would like to acknowledge all the students who assisted me through this work, notably: Jamie Chandler, Joanna Tinnirella, David Griffin and Patrick Elder.

TABLE OF CONTENTS

Page

Chapter 1. INTRODUCTION AND OVERVIEW

1.1 PROBLEM STATEMENT AND PROPOSED APPROACH

Surfactant molecules spontaneously form various types of self-assembled structures in aqueous solution.[1,2] Since self-assembly is controlled by thermodynamics, self-assembled structures will respond to changes in thermodynamic variables such as concentration and temperature. Other external variables such as light and electric fields may also influence the shape and size of the self-assembling molecules, and thereby control their assembly in solution. The goal of this thesis is to exploit the sensitivity of self-assembled structures in developing "smart" fluids or materials that respond in an unusual or interesting way to an external input. Two desirable types of responses are targeted in particular, and these are illustrated in Figures 1.1 and 1.2. In Figure 1.1, the fluid on the left has a low viscosity, but when a "switch" is turned on (e.g., light at a

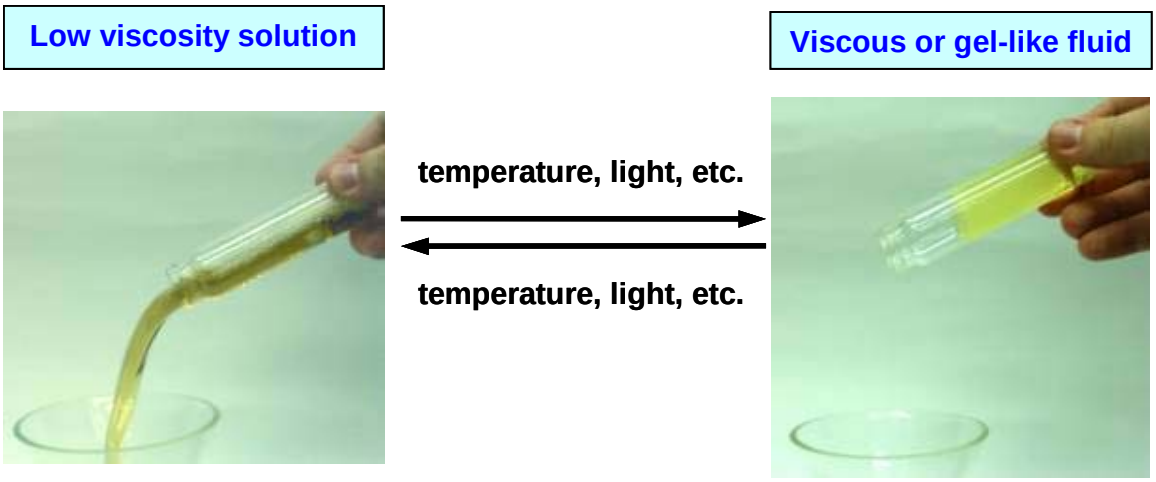

Figure 1.1 Illustration of smart fluids that can reversibly change their viscosity in response to a change in an external input.

given wavelength, or a spike in temperature), it transforms into a highly viscous or gel-like fluid that cannot be poured from the vial. An important characteristic desired out of such smart fluids is their reversibility, i.e., their ability to switch back to their original state. In reference to Figure 1.1, one envisions a second switch (e.g., light at a different wavelength, or a downward spike in temperature) that can make the fluid revert to its original state.

Figure 1.2 illustrates a switching response that is particularly interesting in the context of biomedical applications such as drug delivery.[3] On the left is a small container containing a drug or other molecule. In response to an external input, the container disrupts, allowing its contents to leak out into the surrounding solution. Thereafter, in response to a second stimulus, the container returns to its closed form. Such smart containers may be used to store drugs and release them on demand at a target location. This illustrates the potential of smart materials in emerging applications.

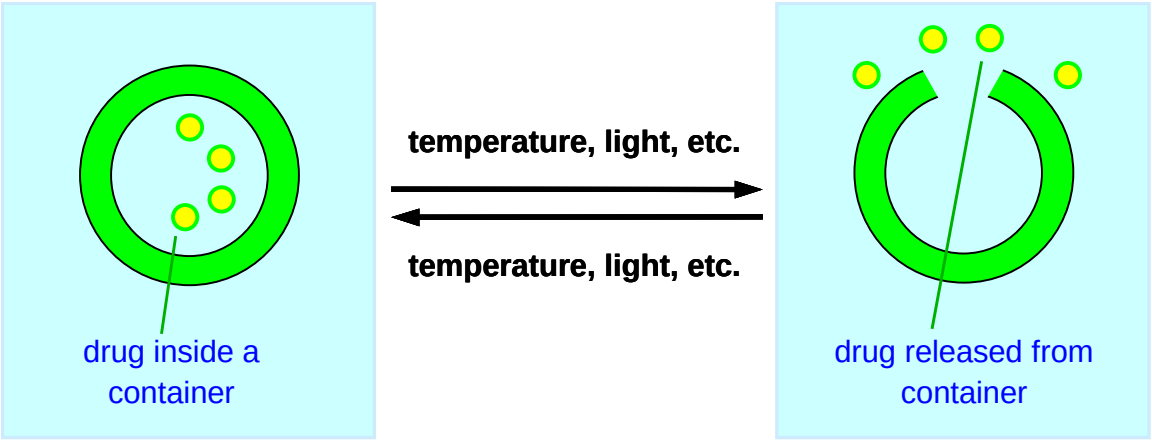

Figure 1.2 Illustration of smart containers that can reversibly break and re-form in response to a change in an external input. This concept can be used to deliver encapsulated molecules.

In this thesis, we will describe a self-assembled system that captures some of the desired attributes discussed above. The system consists of a surfactant and an organic molecule, and mixtures of these molecules self-assemble into two different types of structures in aqueous solution, namely vesicles and micelles. *Vesicles* are a type of self-assembled container where a thin shell of surfactant molecules surrounds a hollow interior composed of water (Figure 1.3).[3] **The main result described in this thesis is that we can induce our vesicles to undergo a reversible transformation into "wormlike micelles" by increasing temperature.** Wormlike micelles are long, cylindrical micellar chains, similar to spaghetti (Figure 1.3).[4,5] Because these chains tend to get entangled with each other, the viscosity of a wormlike micellar solution tends to be very high. Thus, a transition from vesicles to wormlike micelles will have the following consequences:

(i) The disruption of vesicles will cause their contents to spill out into the solution

(ii) The formation of wormlike micelles will increase the viscosity of the solution.

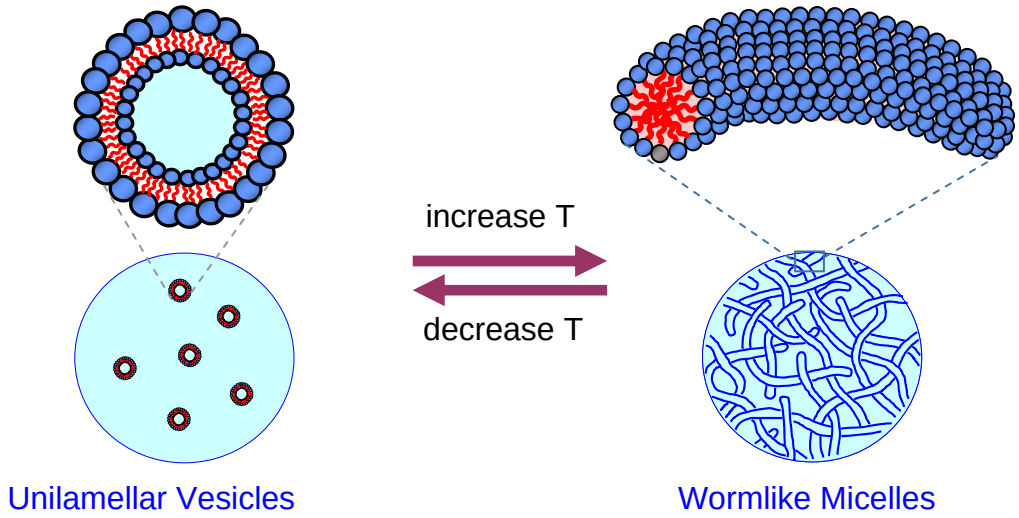

Figure 1.3 Main result from this thesis: vesicle to wormlike micelle transition with increasing temperature in a solution of surfactant (CTAB) and organic acid (5mS).

1.2 SIGNIFICANCE OF THIS WORK

The work described in this thesis deals with several unusual properties of a surfactant fluid. Firstly, the formation of vesicles in this type of a system is itself rare. As discussed in the next chapter, vesicles are usually formed from lipids or in mixtures of two surfactants.[3,6] Secondly, reversible transitions from vesicles to wormlike micelles are also very rare.[7,8] We have only found a few papers in the literature which have described this behavior, and earlier systems were considerably more complicated than the present one. Thirdly, an increase in fluid viscosity with temperature is also quite unusual. As our intuition might suggest, most fluids tend to get less viscous upon heating.[9] Here, we have an instance where the opposite is true – the viscosity of our fluids can increase more than 1000-fold with increasing temperature.

The fluids described here may have some potential utility. Applications may either exploit the reversible disruption of containers (vesicles), or the viscosity increase exhibited by these fluids upon increasing temperature. An example of the first kind would be a biomedical application where vesicles would be used to encapsulate drugs in their aqueous interior. One could then trigger the disruption of these vesicles by increasing the temperature and the released drug would remain embedded in the viscous micellar fluid. Examples where switchable viscosities could find use are in the design of microfluidic valves, in capillary electrophoresis, or in enhanced oil recovery. For instance, hydraulic fracturing operations in oil recovery require the use of a fluid that becomes gel-like at the high temperatures experienced deep inside oil wells.[5] At the same time, a low viscosity at ambient temperatures could enable the fluid to be pumped down easily.

1.3 SCIENTIFIC OBJECTIVES

The focus here is not on finding new applications, but on the underlying science. We are interested in systematically elucidating the properties of our surfactant system as a function of composition and temperature. The questions that we are particularly interested in answering are:

(a) Under what conditions do vesicles form? What are their sizes?

(b) Under what conditions do micelles form? What are their sizes and shapes?

(c) Is the transition from vesicles to micelles a discontinuous or continuous process?

(d) What variables can be tuned so as to control the onset of the above transition?

To answer these questions, we use a variety of techniques, including turbidity measurements, small-angle neutron scattering (SANS) and rheological measurements. The results are described in Chapter 3.

Chapter 2. BACKGROUND

This thesis is concerned with micelles, vesicles and the transitions between these two types of structures. In this chapter, the essential characteristics of these structures are described. Thereafter, the techniques used to study these structures, such as rheology and scattering, are described in brief.

2.1 MICELLES

Micelles are formed by the spontaneous self-assembly of amphiphilic molecules in water.[1] Micelle formation occurs only beyond a critical concentration of the amphiphile, referred to as the critical micelle concentration or cmc. The formation of micelles, as with all self-assembly processes, is governed by thermodynamics, i.e., micelle formation occurs because the system minimizes its Gibbs free energy in the process. The driving force for micellization is the gain in entropy of water molecules when surfactant hydrophobes are removed from their midst and buried in a micelle; this is the hydrophobic effect. Several different shapes are possible for micelles, including spheres, cylinders, and prolate or oblate ellipsoids. At the cmc, most surfactants tend to form spherical micelles, but as the surfactant concentration increases, these micelles can grow into cylinders.[10-13] Micellar geometry can be understood on the basis of a term called the critical packing parameter or CPP, which is defined as follows:[2]

$$\mathrm{CPP} = \frac{a_{\mathrm{tail}}}{a_{\mathrm{hg}}} \tag{1}$$

where a_{hg} is the effective area of the amphiphile headgroup and a_{tail} is the average area of the amphiphilic tail. The larger the headgroup area compared to the tail area, the more curved the aggregate, as shown in Figure 2.1. Thus, a CPP of ⅓, corresponding to a cone shape, leads to spherical micelles while a CPP of ½ (truncated cone) corresponds to cylindrical micelles. Finally, molecules shaped like cylinders, i.e., having $a_{tail} \approx a_{hg}$ and CPP = 1, tend to assemble into bilayer structures (vesicles).

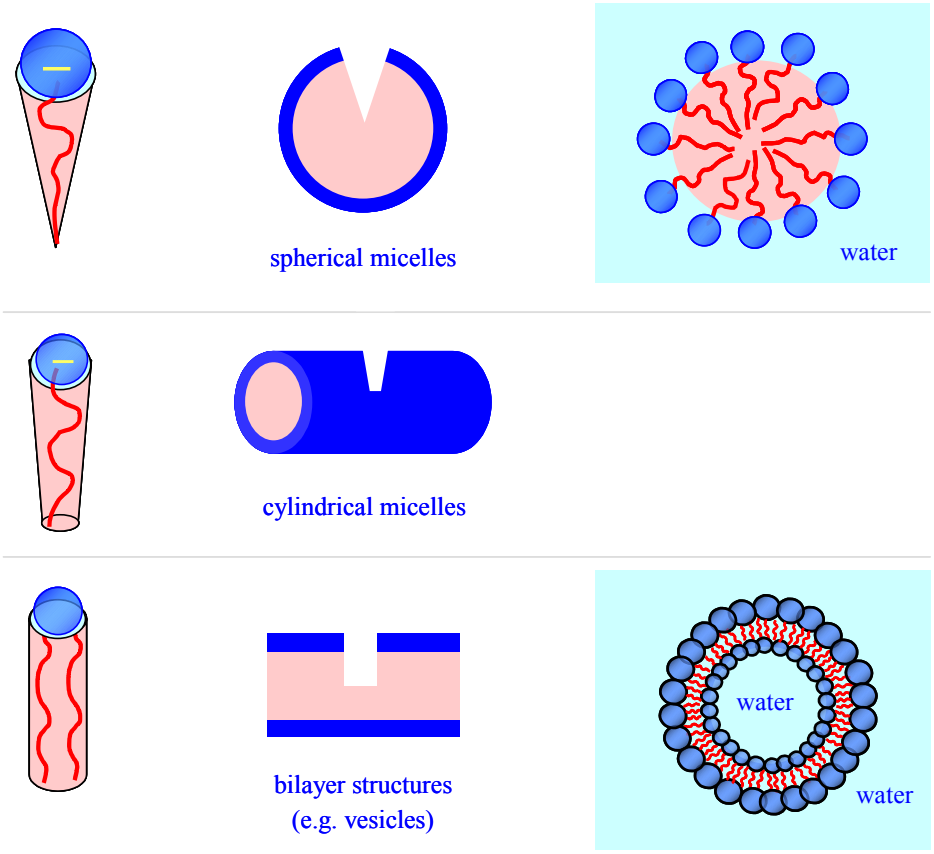

Figure 2.1 Schematics showing the connection between the self-assembly of amphiphiles and their molecular geometry. The hydrophilic heads are shown in blue and the hydrophobic tails in red.

2.2 WORMLIKE MICELLES

Wormlike micelles are long and flexible cylindrical chains with end-to-end lengths up to a few microns (in comparison, spherical micelles usually have a diameter around 5 nm).[4,5,14,15] These micelles are formed by a range of surfactants, but the most popular recipes involve cationic surfactants like cetyl trimethylammonium bromide (CTAB).[15-19] The surfactant CTAB has a 16-carbon tail and a positively charged headgroup. When added to water, CTAB tends to form spherical micelles because the ionic headgroups have a large, effective area due to their electrostatic repulsions. However, when salt is added to CTAB, the added ions screen the repulsions between the cationic headgroups, reducing the headgroup area, and increasing the CPP from ⅓ to ½. As a result, CTAB forms cylindrical micelles that grow uniaxially into long chains.

Wormlike micellar chains are very much like polymer chains and tend to become entangled in solution.[15,20] The entanglement leads to a transient network of chains and this makes the micellar solution highly viscous and viscoelastic. The presence of viscoelasticity manifests in phenomena such as rod climbing and elastic recoil, as well as in the presence of entrapped bubbles in the sample. Another characteristic property of these micellar fluids is their flow birefringence.[15] That is, when a wormlike micellar solution placed in a vial is shaken lightly and observed under crossed polarizers, one observes bright streaks of light in the sample (Figure 2.2). These streaks emerge because the micellar chains tend to become aligned when sheared, thus making the sample anisotropic. Birefringence, which refers to a difference in refractive indices along mutually perpendicular directions, is a characteristic property of anisotropic materials

Figure 2.2 Flow-birefringence in a wormlike micellar solution.

like liquid crystals.[9] Note that wormlike micelles do not exhibit birefringence at rest, but only when subjected to flow or shear.[15]

2.2.1 Effect of Aromatic Salts and Acids on Micellar Growth

As mentioned, the addition of salt to ionic surfactants like CTAB induces the growth of wormlike micelles. However, some salts termed "binding salts" are much more effective than other "simple salts" in this regard.[15] Simple salts refers to strong electrolytes like sodium chloride, NaCl, which merely have a "screening" effect on the electrostatic interactions. In other words, these ions decrease the Debye length κ^{-1}, which mediates the range of electrostatic repulsions between the headgroups. Binding salts, on the other hand, tend to be aromatic moieties such as sodium salicylate (SS). Because the benzene ring is hydrophobic, counterions of these salts will tend to strongly bind to the micellar interface.[21,22] As shown in Figure 2.3, they will embed their benzene ring into

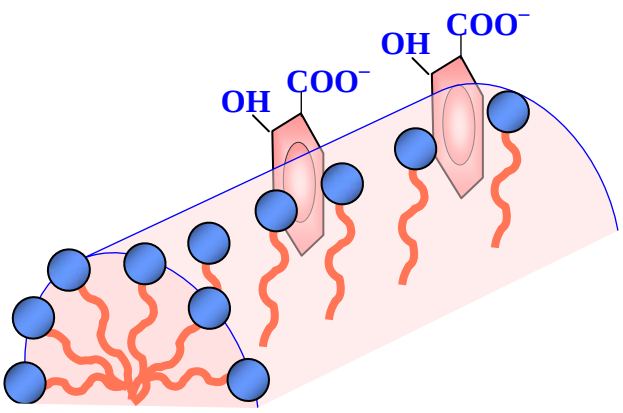

Figure 2.3 Binding of salicylate (o-hydroxy benzoate) counterions to cationic micelles. The aromatic ring is embedded into the hydrophobic interior of the micelle shown in red. The hydrophilic groups (OH and COO^-) protrude out of the micelle.

the hydrophobic interior of the micelle, while at the same time, their negative charge will be localized right next to the positively charged headgroups. Thus, binding salts are very effective at canceling out the surface charge on the micelle, and thereby at mitigating the repulsions between the headgroups. This explains why just millimolar amounts of binding salts have the same effect at inducing micellar growth as ca. 100 mM of NaCl.

A large number of aromatic binding salts have been investigated for cationic micelles.[15] In addition to salicylate, other effective counterions include tosylate, chlorobenzoate, and hydroxy-naphtalene carboxylate. Studies have also been conducted with the acid forms of these salts, and many of these also promote the growth of wormlike micelles.[19,23] For example, salicylic acid has similar effects as sodium salicylate, albeit at slightly higher concentrations. In our studies in Chapter 3, we will employ a closely related derivative, 5-methyl salicylic acid (5mS) as the organic moiety of interest. The growth of micelles in CTAB/5mS mixtures has been studied in detail.[19] In addition to micelles, we will see that 5mS can also induce vesicles in CTAB mixtures.

2.3 VESICLES

Vesicles (or liposomes) are self-assembled containers formed in water by amphiphilic molecules.[3,6] The shell of the vesicle is a bilayer (*ca*. 2-5 nm in thickness) of these amphiphiles, with the hydrophilic heads on both sides of the bilayer and thereby exposed to water, while the hydrophobic tails inside the bilayer are shielded from water (Figure 2.1). A vesicle can be considered to form by the folding of the bilayer into a sphere. Vesicles with only a single bilayer (or lamella) are called unilamellar vesicles (ULVs), whereas vesicles with several concentric bilayers are called multilamellar vesicles (MLVs) or "onions".

As mentioned earlier, vesicles are formed by amphiphiles that roughly have the shape of a cylinder, i.e., a packing parameter close to 1. Such cylinder shapes can be achieved in two main ways, as shown in Figure 2.4, and these represent two ways to form

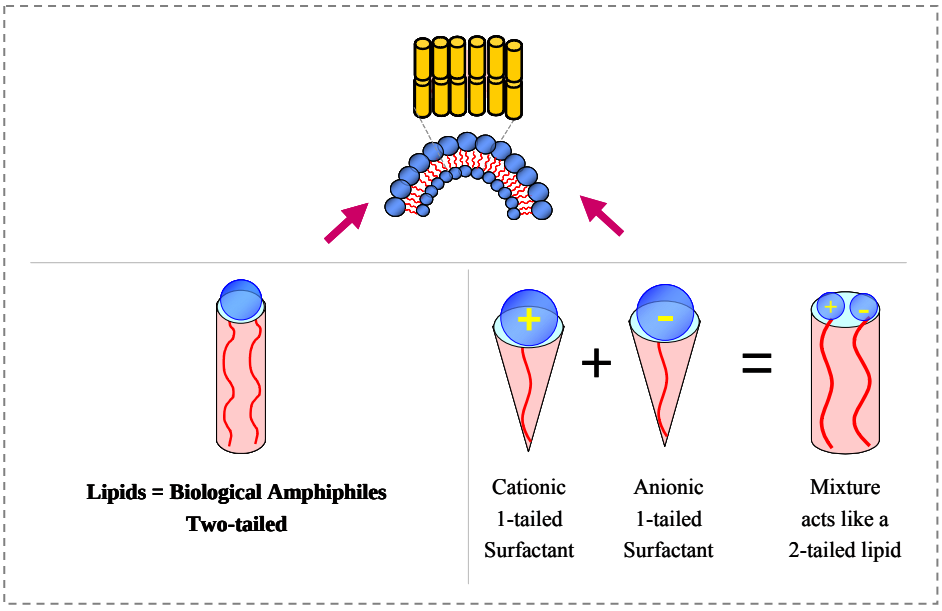

Figure 2.4 Role of geometry in bilayer and vesicle formation. Amphiphiles that have a cylinder-like shape tend to form bilayers. These include lipids (2-tailed biological amphiphiles) as well as mixtures of oppositely-charged single-tailed surfactants.

vesicles. The first is to use amphiphiles with two tails, also called lipids, which often have a biological origin.[3] Cell membranes consist of lipid bilayers. Lipids tend to have a very low solubility in water because of their bulky hydrophobic part. Therefore, to prepare unilamellar lipid vesicles, one requires some input of energy.[3]

The second common way to form unilamellar vesicles is by using two single-tailed amphiphiles, one cationic and the other anionic.[6] The formation of such "catanionic" vesicles can also be understood via the CPP concept, as shown in Figure 2.4. In this case, each individual surfactant molecule resembles a cone because of the electrostatic repulsion from its headgroup. Thus, when present alone, each surfactant would form micelles. When mixed together, however, the cationic and anionic headgroups cancel out their electrostatic effects, causing a significant reduction in their headgroup areas. The combination thus resembles a cylinder and thereby forms vesicles. Interestingly, formation of these vesicles occurs spontaneously when the two surfactants are added into water.[6] Moreover, the vesicles are indefinitely stable, which suggests that they may actually be equilibrium structures.[6]

In Chapter 3, we will discuss a third way to form vesicles, which is by mixing a single-tailed cationic surfactant with an aromatic acid. This approach is similar to the mixtures of surfactants discussed above because the surfactant and the acid tend to bind very strongly. The difference is that only one of the two components in the mixture is a surfactant. The fact that vesicles form in these systems is still not very well known and the vesicle formation process is not fully understood.

2.4 CHARACTERIZATION TECHNIQUE - I: RHEOLOGY

Rheology is defined as the study of flow and deformation in materials.[24] Rheological measurements are useful because they can be correlated with the microstructure in various soft materials.[9,24] These measurements are typically performed under steady or dynamic oscillatory shear. In steady shear, the sample is subjected to a constant shear-rate $\dot{\gamma}$ (e.g. by applying a continuous rotation at a fixed rate on a rotational instrument), and the response is measured as a shear-stress σ. The ratio of shear-stress σ to shear-rate $\dot{\gamma}$ is the (apparent) viscosity η and a plot of this viscosity vs. shear-rate is called the flow curve of the material. In dynamic or oscillatory shear, a sinusoidal strain γ is applied to the sample:[24]

$$\gamma = \gamma_0 \sin(\omega t) \tag{2}$$

where γ_0 is the strain-amplitude (i.e. the maximum applied deformation) and ω is the frequency of the oscillations. The sample response will be a sinusoidal stress σ that will be shifted by a phase angle δ with respect to the strain waveform:

$$\sigma = \sigma_0 \sin(\omega t + \delta) \tag{3}$$

Using trigonometric identities, the stress waveform can be decomposed into two components, one in-phase with the strain and the other out-of-phase by 90°:

$$\sigma = G'\gamma_0 \sin(\omega t) + G''\gamma_0 \cos(\omega t) \tag{4}$$

where G' = **Elastic** or **Storage Modulus**

and G'' = **Viscous** or **Loss Modulus**

The elastic modulus G' is the in-phase component and provides information about the elastic nature of the material. Since elastic behavior implies the storage of deformational energy, this parameter is also called the storage modulus. The viscous modulus G'', on the other hand, is the out-of-phase component and characterizes the viscous nature of the material. Since viscous deformation results in energy dissipation, G'' is also called the loss modulus. For these properties to be meaningful, dynamic rheological measurements must be made in the "*linear viscoelastic*" (LVE) regime of the sample. Over this regime, the stress will be linearly proportional to the imposed strain (i.e., the moduli will be independent of strain amplitude). In that case, the elastic and viscous moduli will be functions only of the oscillation frequency ω. A log-log plot of the moduli vs. frequency, i.e. $G'(\omega)$ and $G''(\omega)$, is called the frequency spectrum or *dynamic mechanical spectrum* of the material. Such a plot is a signature of the microstructure in the sample.[24]

The important advantage of dynamic shear is that it allows us to characterize microstructures without disrupting them. The deformation imposed on the sample is minimal because the experiments are restricted to strain amplitudes within the LVE regime. In other words, the linear viscoelastic moduli reflect the microstructures present in the sample at rest.[24] This is to be contrasted with steady shear, where the material functions are obtained under flow conditions, corresponding to relatively high deformations. We can therefore correlate dynamic rheological parameters to the static microstructure, and parameters under steady shear to flow-induced changes in the microstructure.

2.5 CHARACTERIZATION TECHNIQUE - II: SANS

Scattering techniques are invaluable probes of micro- and nanostructure in soft materials.[25] The principle behind all scattering techniques is that the intensity of scattered radiation is a function of the size, shape, and interactions of the "particles" present in the sample. For aqueous samples, small-angle neutron scattering (SANS) is the technique of choice because contrast between the particles and the solvent can be easily achieved by switching H_2O with D_2O. Also, the incident radiation in SANS is composed of neutrons having a wavelength ~ 6 Å, and therefore SANS is useful in probing size scales on the order of several nm. SANS experiments require a nuclear reactor to generate neutrons and the SANS facilities at the National Institute for Standards and Technology (NIST) in Gaithersburg, MD were used for this work.

Figure 2.5 shows the basic geometry of a SANS experiment. Neutrons at a particular wavelength and wavelength spread are selected using a velocity selector, collimated by several lenses, and then sent through the sample. The scattered neutrons are collected on a 2-D detector. This 2-D data is corrected and placed on an absolute scale

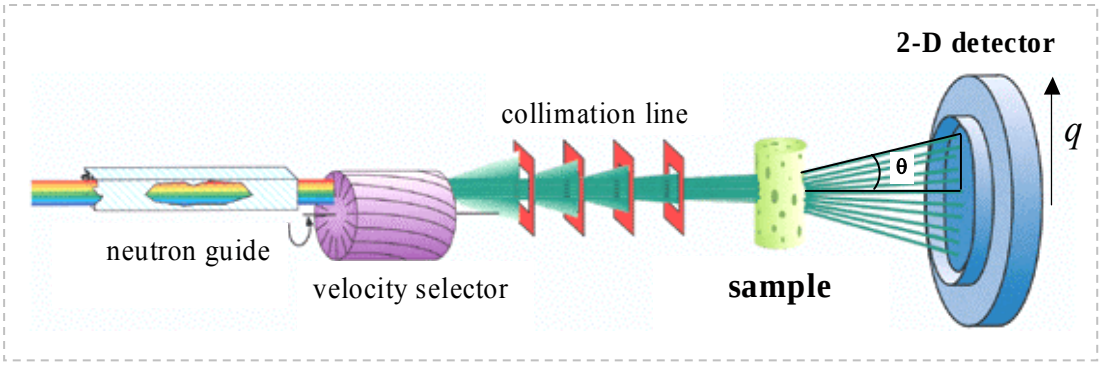

Figure 2.5 Schematic of a SANS experiment (adapted from www.gkss.de).

using calibration standards. It is then converted into a plot of scattered intensity I vs. wave vector q by spherically averaging the data. The wave vector q is related to the scattering angle and wavelength by:[25]

$$q = \frac{4\pi}{\lambda}\sin\left(\frac{\theta}{2}\right) \tag{5}$$

Here, λ is the wavelength of the incident radiation and θ is the scattering angle. q can be considered an inverse length scale, i.e., high q relates to small structures, and vice versa.

The SANS intensity $I(q)$ from a fluid containing n_p particles per unit volume can be expressed in the following manner:[25]

$$I(q) = n_p \cdot P(q) \cdot S(q) \tag{6}$$

where $P(q)$ is the form factor and $S(q)$ the structure factor. $P(q)$ is the scattering that arises from intraparticle interference, which is a function of particle size and shape. $S(q)$ arises from interparticle interactions and is thus related to the spatial arrangement of particles. When the particles are in dilute solution or are non-interacting, the structure factor $S(q) \rightarrow 1$ and $I(q)$ can be modeled purely in terms of the form factor $P(q)$. For scattering from unilamellar vesicles of radius R and bilayer thickness t, the form factor $P(q)$ is given by the following expression, which is valid for thin bilayers ($t << R$):[25]

$$P(q) = (\Delta\rho)^2 \cdot (4\pi R)^2 \cdot \frac{t^2}{q^2}\sin^2(qR) \tag{7}$$

Here ($\Delta\rho$) is the difference in scattering length density between the vesicle bilayer and the solvent and $(\Delta\rho)^2$ is thus a measure of the scattering contrast. Equation 7 indicates that for thin vesicles, $I(q)$ should show a q^{-2} decay in the low q range.

The bilayer thickness t can be obtained by analyzing the intensity at high q using the Guinier approximation for the form factor in this range:

$$q^2 \cdot I(q) \sim t^2 \exp(-q^2 R_t^2) \tag{8}$$

Here, R_t is the radius of gyration for the thickness. This equation shows that a semilog plot of $\ln(Iq^2)$ vs. q^2 will be a straight line with a slope equal to R_t^2 (such a plot is called a cross-sectional Guinier plot). The thickness t is related to R_t by the equation below:

$$t = \frac{R_t}{\sqrt{12}} \tag{9}$$

2.5.1 IFT Modeling of SANS Data

Modeling of SANS data can be done in two ways.[26] In one approach, a certain type of structure is assumed *a priori* to exist in solution and then the appropriate form factor $P(q)$ is fit to the data. For example, if unilamellar vesicles were assumed to be present, one could fit eq 7 to the data, and thereby obtain the bilayer thickness t and the vesicle radius R. The disadvantage of this approach is that a good fit to the data does not necessarily mean our assumption was correct, i.e., many models could fit the same data, especially if they had a large number of variable parameters. One also has to make assumptions as to whether the structures present are monodisperse or polydisperse – the form factor models are different and more complicated for the polydisperse case.

The deficiencies with the "straight modeling" approach have led to the development of an alternate method of analysis that requires no *a priori* knowledge about the scatterers.[26,27] This is the Indirect Fourier Transform (IFT) method, and here a Fourier

transformation is done on the scattering intensity $I(q)$ to give the pair distance distribution function $p(r)$ in real space. $I(q)$ and $p(r)$ are related by the following equation:[26]

$$I(q) = 4\pi \int_0^\infty p(r) \frac{\sin(qr)}{qr} dr \tag{10}$$

The $p(r)$ function provides structural information about the scatterers in the sample. In particular, the largest dimension of the scattering entities can be estimated. Typical $p(r)$ functions for spherical micelles, cylindrical micelles, and unilamellar vesicles are shown in Figure 2.6. Note that this IFT analysis is valid only for non-interacting scatterers.[26] Before implementing the IFT methodology, it is useful to first subtract the incoherent background from the scattering data. This background can be estimated from the asymptotic slope of a Porod plot ($I(q)\cdot q^4$ vs. q^4). A software package is commercially available to perform the IFT calculation on the data with subtracted background.

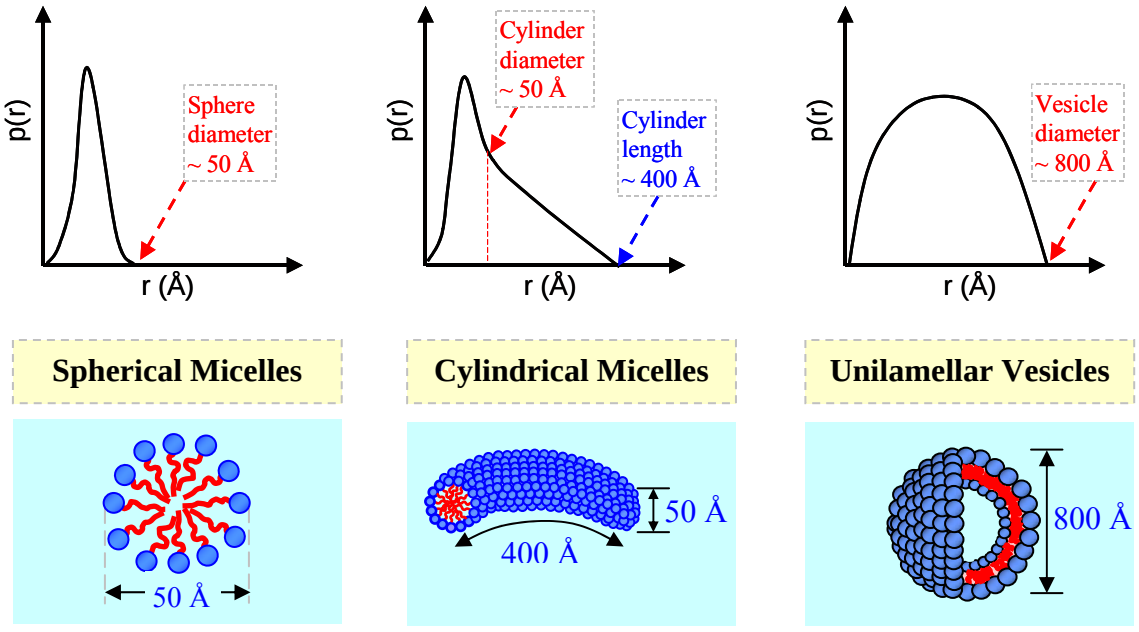

Figure 2.6 Expected $p(r)$ functions for different self-assembled structures. The relevant sizes are correlated with points on the respective $p(r)$ plots.

Chapter 3. VESICLE – MICELLE TRANSITIONS IN THE CTAB/5MS SYSTEM

3.1 INTRODUCTION AND PREVIOUS WORK

In this chapter, we describe our findings on mixtures of the cationic surfactant, cetyl trimethylammonium bromide (CTAB) and the aromatic derivative, 5-methyl salicylic acid (5mS). We use visual observations, turbidimetry, rheological techniques, and small-angle neutron scattering (SANS) in our studies. Two principal results are obtained from this work: (i) we show that CTAB/5mS mixtures can form either wormlike micelles or unilamellar vesicles depending on the composition of the mixture; and (ii) we also demonstrate that the vesicular solutions can be transformed into wormlike micellar fluids upon heating, resulting in a dramatic (1000-fold) increase in the viscosity of the sample. We will show that the vesicle to micelle transition is a reversible and continuous (second-order) phase transition, and that its onset is tunable. The above results are unusual and atypical for these types of surfactant mixtures and we will propose a tentative hypothesis to explain their occurrence in the CTAB/5mS system.

In Chapter 2, we had discussed the two typical methods for forming vesicles: (a) using two-tailed lipids, and (b) by mixing one-tailed cationic and anionic surfactants (Figure 2.4, Section 2.3). In contrast to lipid vesicles, the catanionic surfactant vesicles were described as "equilibrium" structures, i.e., they are stable for very long periods of time. The system studied here has some similarities to the catanionic systems – here,

instead of two surfactants, we employ one cationic surfactant and an aromatic acid that becomes negatively charged when ionized. Mixtures of cationic surfactants with aromatic salts and acids have been extensively studied.[15,19,23] As discussed in Section 2.1, the addition of a binding aromatic salt like sodium salicylate to cationic spherical micelles, induces the growth of these micelles from spheres to wormlike chains.[15] Similar micellar growth can also be induced by acids, although their solubility in water is low compared to the salts.[19,23] The mechanism for micellar growth involves a change in the packing parameter from about 1/3 (spheres) to 1/2 (cylinders) due to the screening of headgroup charge by the bound aromatic molecules (Figure 2.3). A further increase in packing parameter from 1/2 to about 1 would lead to the formation of bilayers (vesicles). Although this seems plausible, reports of vesicles in mixtures of surfactants and aromatic derivatives are actually rare.

A few relevant studies are worth discussing. Mixtures of CTAB and 5mS have been previously studied by Davis *et al*.[19] The focus of their study was on the structural transition from spherical to wormlike micelles as the 5mS:CTAB molar ratio was increased from zero to beyond equimolar. Surprisingly, at a molar ratio around 1.1, the authors found instead that their solution contained unilamellar vesicles. This result was inferred from a cryo-transmission electron microscopy (cryo-TEM) image, which showed vesicles around 100 nm in diameter. Detailed investigations of vesicle formation were not reported in this study. In a subsequent paper, Davis, Zakin and co-workers[28] again used cryo-TEM to infer the presence of vesicles, this time in mixtures of CTAB and the

sodium salt of 3-methyl salicylic acid (3mS). These vesicles were reported to transform into cylindrical micelles upon shearing.

Few reports exist in the literature on vesicle to wormlike micelle transitions with increasing temperature.[7,8] In the system studied by Manohar et al.,[7] the surfactant was obtained by mixing equimolar amounts of CTAB with sodium 3-hydroxynaphtalene 2-carboxylate (SHNC), followed by removal of excess counterions. This surfactant when added to water at room temperature assembled into multilamellar vesicles (MLVs) around 1 – 10 μm in diameter.[7] Due to the formation of these large MLVs, the solutions were highly turbid and quite viscous (viscosities ca. 100 times that of water). Upon increasing the temperature, the samples transformed into clear solutions containing wormlike micelles, thereby leading to an increase in viscosity by about an order of magnitude.[7] It is not clear if the MLVs in these samples at low temperatures were stable or if they aggregated and eventually phase-separated to form a lamellar phase.

The present study with the CTAB/5mS system began in an attempt to reproduce the result of Davis *et al.*[19] in terms of forming unilamellar vesicles. Subsequently, we detected by visual observation a dramatic increase in viscosity when some of these samples were heated. This prompted us to carry out a systematic study of CTAB/5mS mixtures over a range of compositions and temperatures and using a variety of techniques. Our results unambiguously demonstrate a transition in these fluids from unilamellar vesicles to wormlike micelles, which in turn leads to a much higher increase in viscosity compared to the earlier reports cited above.

3.2 MATERIALS AND METHODS

Materials and Sample Preparation. CTAB from Sigma-Aldrich and 5-methyl salicylic acid from TCI America were of > 98% purity and were used as received. Solutions were prepared by adding ultra-pure deionized water from a Millipore water-purification system into weighed quantities of the relevant compounds. The samples were heated to ~ 65ºC under continuous stirring for approximately an hour till the solutions became homogeneous. They were then left to cool overnight while being stirred before any further experimentation. For SANS studies, samples were prepared using the same methods, but with the solvent being D_2O (99.95% D, purchased from Cambridge Isotope Laboratories, Andover, MA).

Phase Behavior. Phase behavior as a function of temperature was determined by visual observation of sealed samples placed in a water bath, where the temperature was controlled by a Julabo^{TM} heater. The transition temperature was recorded as the point at which the sample became completely transparent. These numbers matched well with values from turbidity measurements.

Turbidity Measurements. Turbidimetric measurements of the solutions were carried out using a Varian Cary 50 UV-Vis spectrophotometer equipped with a thermostated cell holder controlled by a Peltier system. The temperature in the sample was double checked using a thermocouple immersed in the sample and placed right above the beam path. Samples were studied in 1 cm cuvettes and the optical density was measured at a wavelength where neither the CTAB nor the 5mS had any measurable absorption.

Solubility Studies. The solubility of 5mS in water at different temperatures was determined as follows. An excess of 5mS was added to water in a 1 cm cuvette and the sample was centrifuged for 15 minutes to compact the 5mS to the bottom of the cuvette. The cuvette was then placed in the thermostated holder of the UV-Vis instrument. The sample was monitored till the absorbance reached a plateau, and this absorbance was converted to a concentration value using the absorbtivity determined from a calibration curve. The same procedure was repeated at different temperatures.

Rheological Studies. Steady and dynamic rheological experiments were performed on an AR2000 stress controlled rheometer (TA Instruments, Newark, DE). Samples were run on a cone-and-plate geometry (40 mm diameter, 2º cone angle) or a couette geometry (rotor of radius 14 mm and height 42 mm, and cup of radius 15 mm). Dynamic frequency spectra were obtained in the linear viscoelastic regime of each sample as determined by dynamic stress-sweep experiments.

SANS. SANS measurements were made on the NG-1 (8 m) beamline at the National Institute of Standards and Technology (NIST) in Gaithersburg, Maryland. Samples were studied at various temperatures in 2-mm quartz cells. Scattering spectra were corrected and placed on an absolute scale using calibration standards provided by NIST. The data is presented as plots of the radially-averaged absolute intensity I versus the wave vector $q = (4\pi/\lambda)\sin(\theta/2)$, where λ is the wavelength of the incident neutrons and θ is the scattering angle. IFT analysis of the SANS data was implemented using the PCG software package.

3.3 RESULTS

3.3.1 Studies at Room Temperature

We begin by discussing the phase behavior of CTAB/5mS mixtures at room temperature (25°C) at a fixed CTAB concentration of 12.5 mM. Figure 3.1 shows two types of data, the zero-shear viscosity η_0 from steady-shear rheology and the optical density, as a function of 5mS concentration, denoted by [5mS]. The optical density was recorded at 400 nm where CTAB and 5mS have no absorption, so that any changes in this quantity are due to the scattering of light.

Consider first the results for [5mS] < ca. 15 mM. At low [5mS] (< 5 mM), the sample is a clear solution with low optical density, and the viscosity is also low, approaching that of water (*ca*. 1 mPa.s). As [5mS] is increased, the viscosity grows by five orders of magnitude. The resulting samples are clear, viscous solutions and show an ability to trap bubbles for long periods of time (see photograph). These samples also exhibit flow-birefringence, i.e., streaks of light appear when a sample viewed under crossed polarizers is shaken lightly (Section 2.2). Both the high viscosity and the flow-birefringence are typical characteristics of wormlike micelles. We can conclude that the addition of 5mS induces the growth of micelles, which is as expected for these salicylic acid derivatives.[19] With further increase in [5mS], the viscosity reaches a peak and thereafter drops precipitously. Similar viscosity peaks are ubiquitous in the wormlike micelle literature, and are believed to signify a transition from linear to branched wormlike micelles.[15]

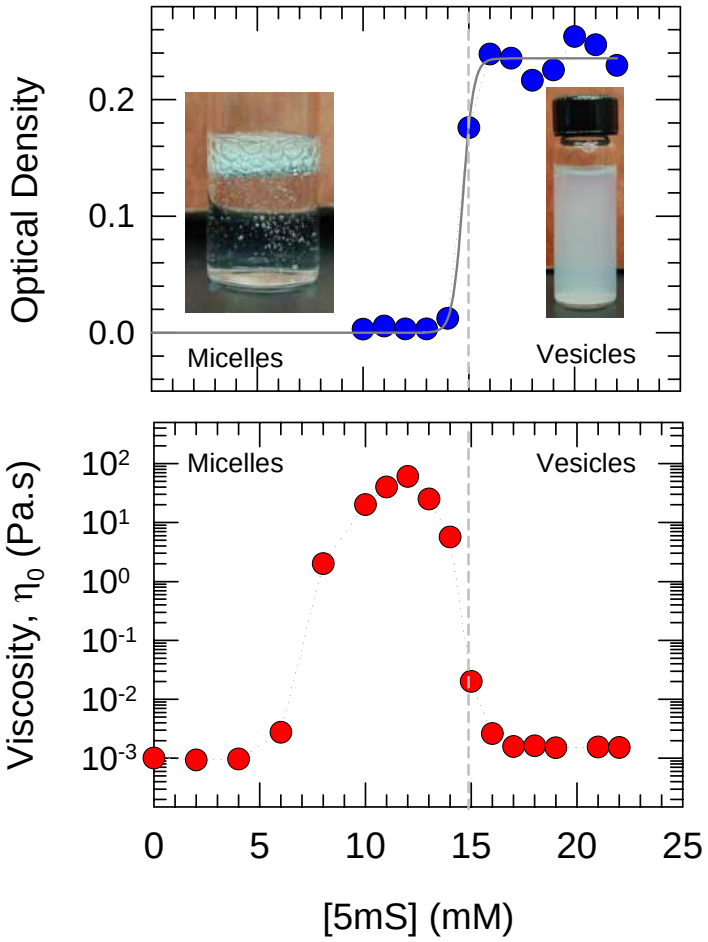

Figure 3.1 Phase behavior at 25°C of CTAB/5mS mixtures at a fixed CTAB concentration of 12.5 mM and varying concentrations of 5mS. The plot on top shows the optical density, which quantifies the amount of light scattered from the sample. The bottom plot shows the zero-shear viscosity obtained from steady-shear rheology. Around ca. 10 mM 5mS, samples are colorless and highly viscous, and show a tendency to trap bubbles (see photograph on left). Beyond ca. 15 mM 5mS, samples have a low viscosity akin to water, and appear bluish due to light scattering, as seen from the photograph on the right.

The unusual aspect is the sample behavior for [5mS] above ca. 15 mM. These samples are homogeneous solutions with a bluish hue (see photograph in Figure 3.1) and with a low viscosity close to that of water. The appearance of the bluish color is typically a manifestation of the Tyndall effect due to large scatterers in solution.[1] Such bluish

solutions are routinely observed in mixed surfactant systems when these form unilamellar vesicles.[6] The onset of the bluish color coincides with the sharp rise in optical density in Figure 3.1. At higher [5mS] the optical density reaches a plateau. Taken together, the data provide preliminary evidence for a phase transition from micellar structures to vesicles. Note that Figure 3.1 extends only up to ca. 23 mM [5mS], which represents a solubility limit for 5mS in water at room temperature in the presence of 12.5 mM CTAB. As mentioned earlier, organic acids like 5mS are sparingly soluble in water. In the absence of surfactant, the solubility of 5mS was measured to be about 7.4 mM.

To further elucidate the microstructures in these samples, we turned to SANS. CTAB/5mS samples were prepared in D_2O to achieve the needed contrast between the structures and the solvent. Samples in D_2O were visually and rheologically identical to the samples prepared with H_2O. Figure 3.2 shows SANS spectra (I vs. q) for 12.5 mM CTAB samples containing different amounts of 5mS. The data for low [5mS] (5 and 10 mM) asymptote to a plateau at low q and essentially correspond to micelles. In contrast, for the higher [5mS] (15 and 20 mM), there is no plateau, but instead a q^{-2} decay of the intensity at intermediate q. Such a decay is a signature of scattering from bilayers (e.g., vesicles) (as discussed in Section 2.5). It is important to point out that the appearance of the q^{-2} decay in SANS coincides with the onset of the vesicle region in Figure 3.1 (i.e., the appearance of bluish, nonviscous samples). Thus, the SANS data corroborates our hypothesis of a phase transition from micelles to vesicles with increasing [5mS]. Further analysis of the SANS data is described later in this section.

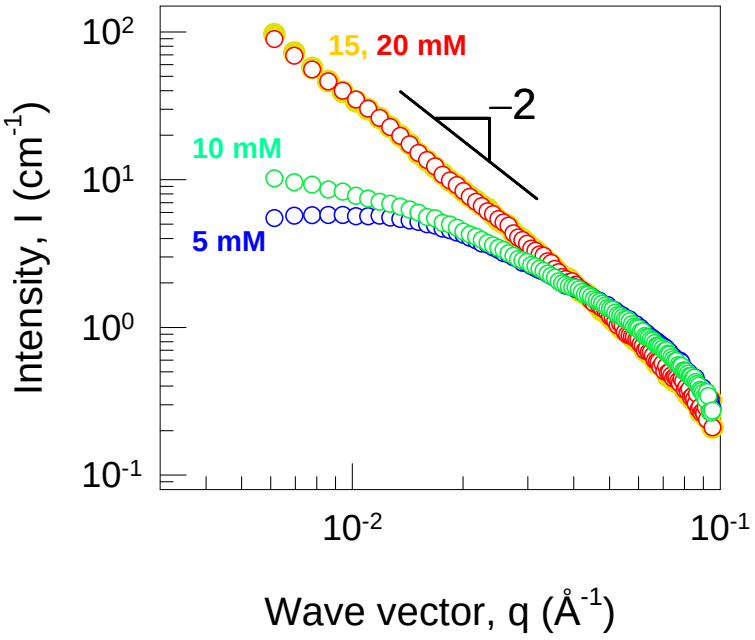

Figure 3.2. SANS scattering at 25°C from CTAB/5mS mixtures at a fixed CTAB concentration of 12.5 mM and varying concentrations of 5mS. Beyond ca. 15 mM 5mS, the data follows a slope of –2 on the log-log plot, which is indicative of scattering from vesicles.

3.3.2. Studies as a Function of Temperature

We have shown that certain CTAB/5mS mixtures contain vesicles. Next, we describe the unusual behavior exhibited by these solutions upon heating, which is evident even by visual observation. The solutions are observed to transform from bluish non-viscous solutions to colorless, perceptibly viscous and flow-birefringent samples. Systematic studies as a function of temperature with a sample containing 12.5 mM CTAB and 20 mM 5mS are reported in Figure 3.3. Here again, both the optical density and the zero-shear viscosity η_0 are shown, this time as a function of temperature. Note that this sample falls in the vesicle region of the phase diagram at 25°C, and at low temperatures (between 25 to ca. 48°C) it remains bluish and scatters light strongly. Around 48°C, the

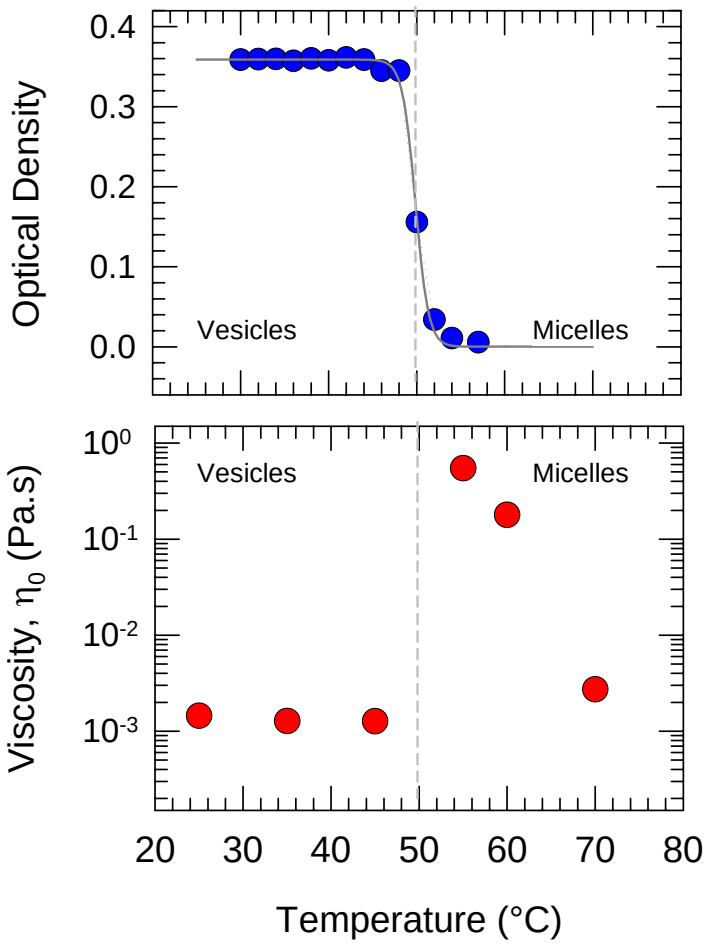

Figure 3.3 Phase behavior vs. temperature of a sample containing 12.5 mM CTAB and 20 mM 5mS. The optical density (top) and the zero-shear viscosity (bottom) are shown. The sharp increase in viscosity and the corresponding decrease in optical density suggest a vesicle-to-micelle transition with increasing temperature.

bluish color slowly begins to fade and the sample transforms to a clear, colorless solution. In turn, the optical density drops sharply and falls to nearly zero by about 54°C. Corresponding changes also occur in the rheology – as the sample clears, it also becomes more viscous, and the zero-shear viscosity η_0 increases by a factor of about 500. At higher temperatures, the sample continues to remain clear and viscous, while the viscosity drops with temperature. These observations suggest a transition from vesicles to wormlike micelles upon heating and we will presently use rheology and SANS to confirm such a transition.

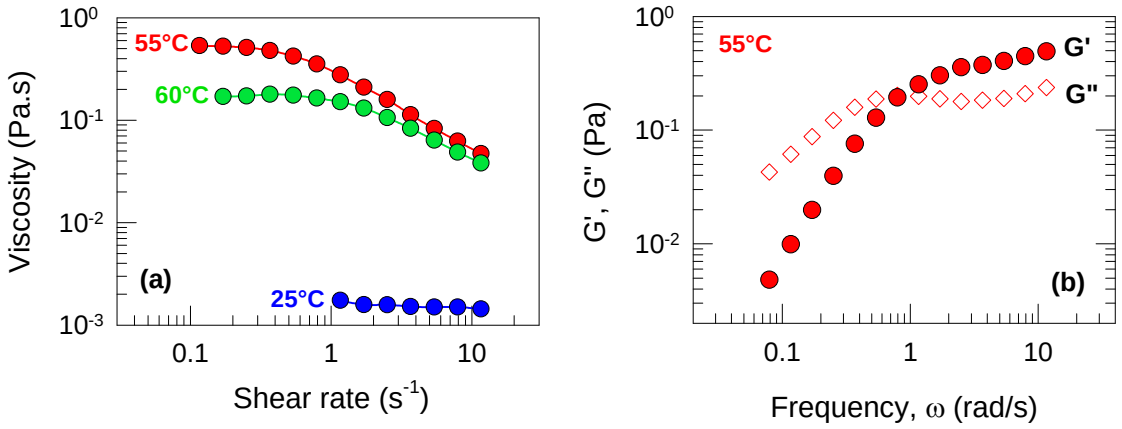

Figure 3.4 Rheology of a 12.5 mM CTAB + 20 mM 5mS sample at various temperatures. The steady-shear rheological response at three different temperatures is shown in (a) and the dynamic rheological response at 55°C is shown in (b).

The rheological response of the above CTAB/5mS sample at various temperatures is shown in Figure 3.4. At low temperatures, the sample contains vesicles and it exhibits a Newtonian response i.e., its viscosity is independent of shear rate (Figure 3.4a). The sample viscosity is close to that of water and it remains at this value from 25 to ca. 50°C. At ca. 55°C, the vesicles are transformed into wormlike micelles, and the sample switches to a shear-thinning response, i.e., there is a plateau in the viscosity at low shear-rates, followed by a drop in viscosity at higher shear-rates. Note also that the zero-shear viscosity is orders of magnitude higher at this temperature. The corresponding dynamic rheological response at 55°C is plotted in Figure 3.4b. Here, the elastic and viscous moduli, G' and G'', are shown as functions of frequency ω. The sample shows a viscoelastic response typical of wormlike micelles – i.e., at high frequencies (or short timescales), it responds elastically ($G' > G''$) while at low frequencies (or long timescales), it switches to a viscous behavior ($G'' > G'$, with both moduli varying strongly with frequency). The longest relaxation time of the sample (inverse of the frequency at

which G' and G'' cross) is about 1.4 s at 55°C. Figure 3.4a also shows that heating the micellar solution from 55 to 60°C lowers the zero-shear viscosity by a factor of 2 (the relaxation time in dynamic rheology is lowered by a similar amount; data not shown). Such a decrease in viscosity and relaxation time with temperature are expected for wormlike micelles – they arise due to an exponential reduction in the micellar contour length with increasing temperature.[15]

Similar temperature-induced changes in both the phase behavior and rheology were observed for all the vesicle samples investigated. The onset of the vesicle to micelle transition, and thereby the onset of the viscosity increase, could be tuned by varying the solution composition. Figure 3.5 plots the transition temperature as a function of [5mS] for a fixed [CTAB] of 12.5 mM. These transition temperatures were determined by visual inspection, and they correlate well with the complete disappearance of turbidity in the sample (i.e., with optical density $\rightarrow$ 0 in plots like Figure 3.3). We note from Figure 3.5 that the phase transition systematically shifts to higher temperatures with increasing

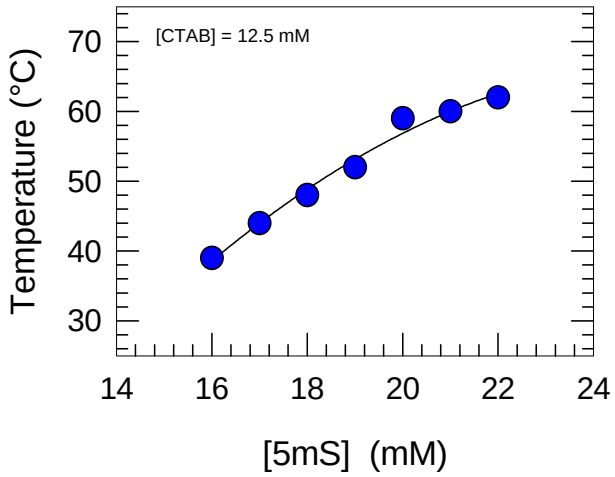

Figure 3.5 Vesicle-micelle phase transition temperature as a function of [5mS] for a fixed concentration of CTAB (12.5 mM).

[5mS]. It is worth emphasizing also that these transitions are thermoreversible, so that vesicles that are disrupted into micelles upon heating are re-formed upon cooling.

Figure 3.6 shows the changes in zero-shear viscosity as a function of temperature for three different CTAB/5mS samples, each with 12.5 mM [CTAB] and differing [5mS]. The data again demonstrate that the onset of the transition, and correspondingly the location of the viscosity peak, shift to higher temperatures as [5mS] is increased. In addition, the *magnitude* of the viscosity rise is also seen to be a function of [5mS]. Thus, the peak viscosity is highest for the 18 mM sample and the viscosity rise in this case amounts to a factor of about 1500. The viscosity rise is less appreciable for the 20 mM sample and an even smaller viscosity increase occurs for the 23 mM one. Similar trends can also be obtained by varying the CTAB concentration in the sample. To sum up, the onset and magnitude of the viscosity increase can be tuned via the sample composition.

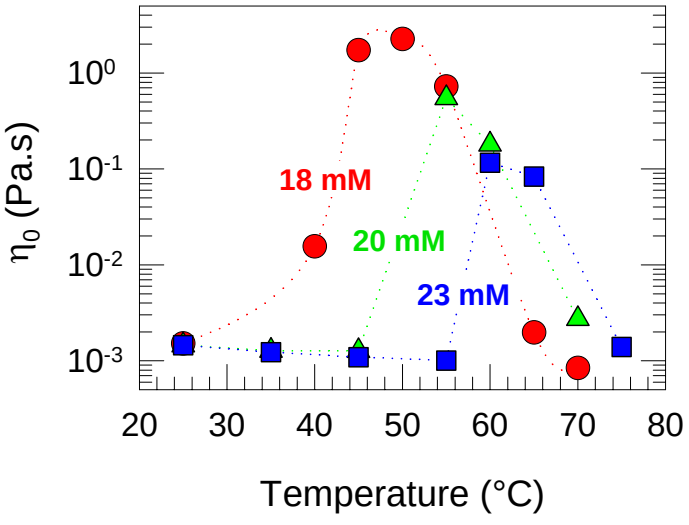

Figure 3.6 Zero-shear viscosity η_0 as a function of temperature for three CTAB/5mS solutions containing 12.5 mM CTAB and differing concentrations of 5mS (indicated along each curve).

Changes in solution structure with temperature were also investigated by SANS. Figure 3.7 shows SANS spectra over a range of temperatures for a sample in D_2O containing 12.5 mM CTAB and 20 mM 5mS. This D_2O sample behaves almost identically as its counterpart in H_2O (Figure 3.3). SANS spectra for this sample overlap perfectly from 25 to 45°C indicating negligible changes in microstructure over this range of temperatures. The data at 45°C are plotted in Figure 3.7 and the characteristic q^{-2} decay of vesicles is seen. Beyond 45°C, however, significant changes occur in the spectra, especially at low q. The intensity drops at low q, and the q^{-2} decay is no longer observed. The onset of changes in SANS coincides with the onset of transitions in turbidity and rheology (Figure 3.3). Thus SANS again confirms the occurrence of a vesicle to micelle transition with increasing temperature in CTAB/5mS samples.

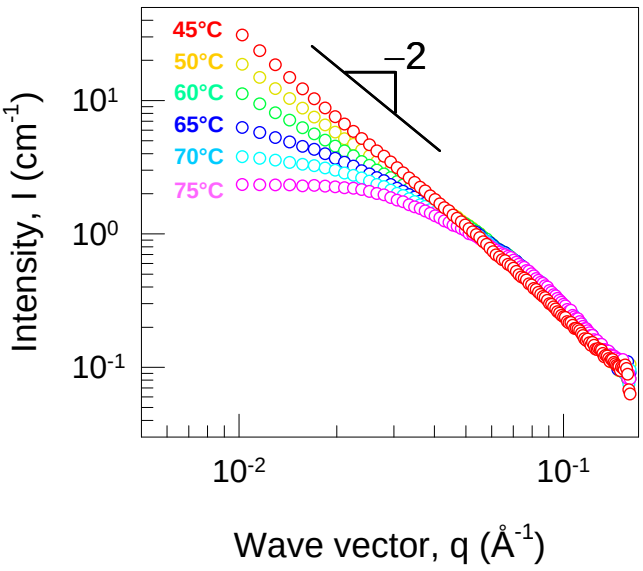

Figure 3.7 SANS scattering at various temperatures from a CTAB/5mS solution containing 12.5 mM of CTAB and 20 mM of 5mS. The data reflect the presence of vesicles at low temperatures (slope of –2) and micelles at higher temperatures.

3.4 DISCUSSION

3.4.1 SANS Modeling

Further information from the SANS data can be obtained by modeling it through the Indirect Fourier Transform (IFT) method, described in Section 2.5.1. Using this method, the SANS data can be analyzed without assuming *a priori* if micelles or vesicles are present in the sample. First, we apply the IFT analysis to the SANS data obtained at room temperature (25°C) (which was presented in Figure 3.2). The pair distance distribution function $p(r)$ from IFT is shown for 5mS concentrations of 10 and 20 mM in Figure 3.8. In this analysis, interactions between the scatterers are ignored. For the 10 mM sample, $p(r)$ is asymmetrical, with an inflection point around 52 Å followed by an approximately linear decrease to zero around 200 Å. This $p(r)$ function is characteristic of cylindrical micelles.[27,29] The inflection point gives the cylinder diameter, while the point

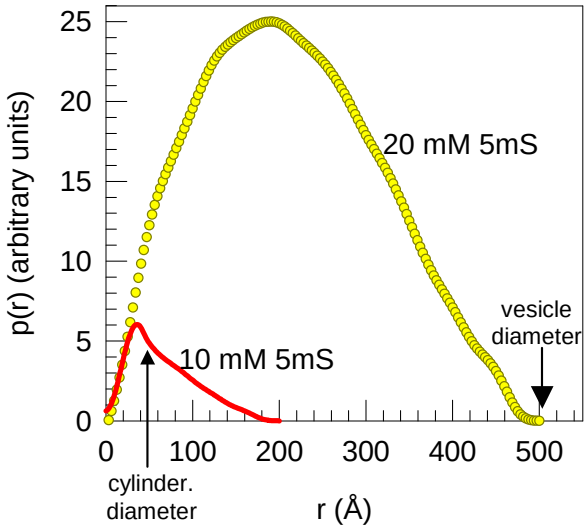

Figure 3.8. Pair distance distribution functions $p(r)$ corresponding to the SANS data at room temperature for CTAB/5mS samples with 12.5 mM CTAB and two different 5mS concentrations (original data in Figure 3.2)

where $p(r)$ meets the axis is an estimate for the overall length of the cylinders.[29] Next, consider the $p(r)$ for the 20 mM sample. This symmetrical $p(r)$ function suggests large spherical structures, i.e., vesicles.[30] Note that the $p(r)$ function for vesicles and micelles are quite different. The point where $p(r)$ meets the axis gives the vesicle diameter in this case, which is about 500 Å. The vesicle bilayer thickness can be determined from the SANS data using a cross-sectional Guinier plot.[25] This semi-log plot of $\ln(Iq^2)$ vs. q^2 falls on a straight line for bilayers, the slope of which is related to the bilayer thickness (Section 2.5). For the 20 mM sample at room temperature (data not shown), the bilayer thickness was calculated from the slope of the straight line in the cross-sectional Guinier plot to be 24.9 Å. This value is comparable to the bilayer thicknesses reported for mixed surfactant vesicles.[6]

Similar IFT analysis was also done on the SANS data as a function of temperature for the 12.5/20 CTAB/5mS sample (presented earlier in Figure 3.7). Corresponding plots of $p(r)$ at the various temperatures are shown in Figure 3.9. At low temperatures (25°C to 45°C), the $p(r)$ is symmetrical and indicative of vesicles. On the other hand, at high temperatures (65°C to 75°C), the $p(r)$ is asymmetrical and corresponds to cylindrical micelles. Between 50 to 60°C, the $p(r)$ plots cannot be classified as either micelles or vesicles alone; instead features of both these structures can be seen. At 50°C, a shoulder appears in the data, which becomes a separate peak by 60°C. Two peaks in $p(r)$ implies the co-existence of two distinct structures.[26] Thus, the IFT analysis reveals that over a span of temperatures, vesicle structures co-exist with the micelles. It is only at higher temperatures that the vesicles are completely disrupted.

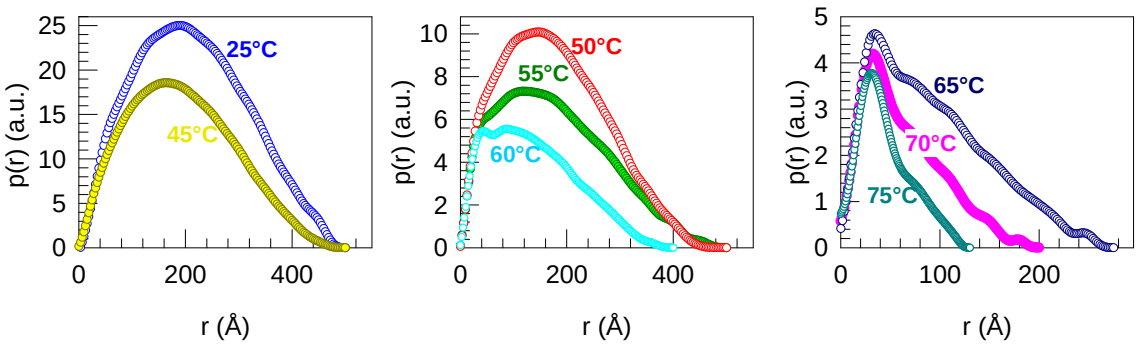

Figure 3.9 Pair distance distribution functions $p(r)$ corresponding to the SANS data at various temperatures for a CTAB/5mS sample with 12.5 mM CTAB and 20 mM 5mS (original data in Figure 3.7).

3.4.2 Implications for the Nature of the Phase Transition

The above analysis has important implications for the nature of the vesicle to micelle phase transition. Based on the IFT plots, this transition is seen to be a continuous (second-order) phase transition. Thus, at the onset of the transition, some of the vesicles are transformed into micelles. As temperature is increased, a larger fraction of vesicles undergo this transformation, i.e., the ratio of micelles to vesicles keeps increasing. This continues until all the vesicles are eventually transformed. The above findings are in broad agreement with earlier studies on vesicle to (spherical) micelle transitions induced by compositional or temperature changes.[31-35] These studies have all found that vesicles and micelles can co-exist at equilibrium under certain conditions. It should be stressed that co-existence does occur at equilibrium, i.e., it is not caused by a slow kinetics of the process.[32,34] Also, unlike typical liquid phases, vesicles and micelles can co-exist without the sample showing a macroscopic phase separation.

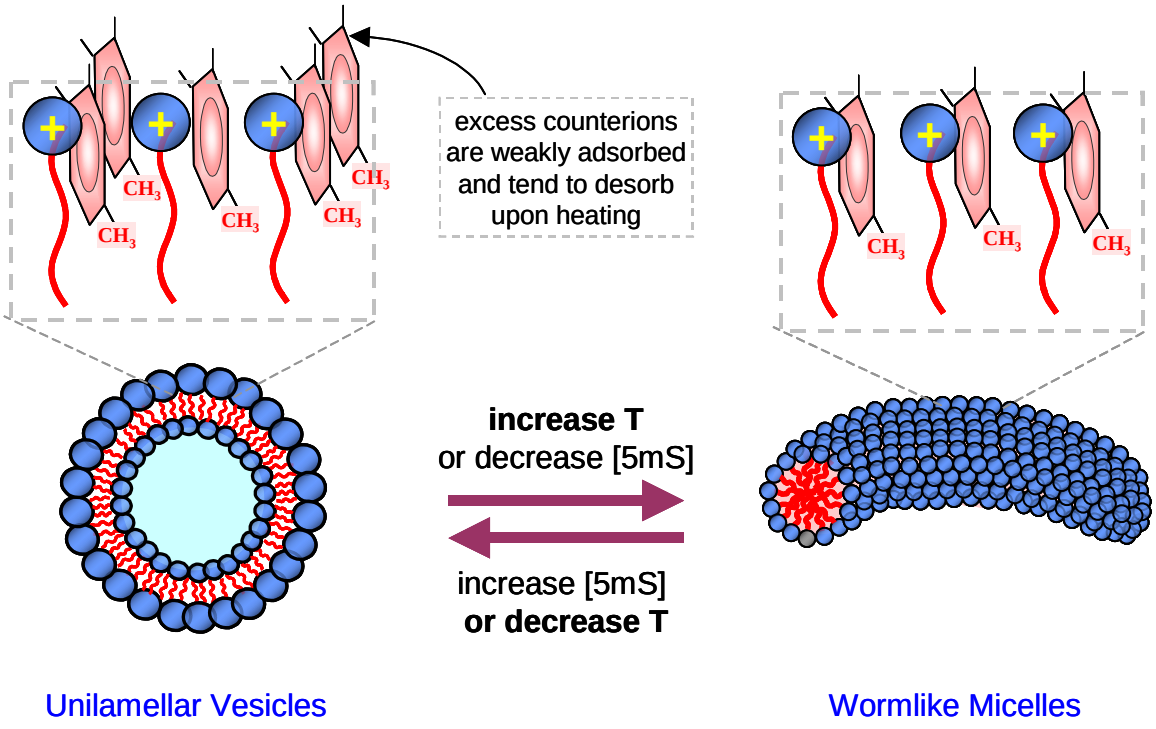

Figure 3.10 Mechanism of the vesicle to wormlike micelle transition in CTAB/5mS systems. Vesicles are formed when there is an excess of 5mS counterions. Some of these counterions will be weakly adsorbed at the aggregate interface and will tend to desorb upon heating. The desorption-induced change in the molecular geometry will induce the system to form wormlike micelles. (Note: the –OH and –COOH groups on 5mS are omitted for clarity.)

3.4.3 Mechanism for the Vesicle-to-Micelle Transition

We now consider the questions of (a) why vesicles form in CTAB/5mS mixtures; (b) why the vesicles become micelles upon heating; and (c) what controls the onset of the transition. A possible mechanism is offered here on the basis of the schematics shown in Figure 3.10. First of all, the 5-methyl salicylic acid molecule will have a strong tendency to bind to the amphiphilic aggregate.[19] This binding will be stronger than that of the parent salicylic acid because of the presence of the methyl group and its location at the 5-position. Being at the 5-position, the methyl group can become embedded in the

hydrophobic part of the aggregate even as the hydrophilic (OH and COO^-) groups at the opposite end of the counterion remain in contact with water. Thus, the 5mS counterion gains an extra binding affinity from the hydrophobic effect on account of the methyl group. The resultant binding of 5mS to CTAB will initially promote the growth of wormlike micelles.[19] However, when the 5mS:CTAB ratio increased beyond equimolar, the packing parameter will be sufficiently increased that the molecules can form vesicles. Note that in our experiments, vesicle formation is initiated for 12.5 mM CTAB when [5mS] increases beyond 15 mM (i.e., slightly above equimolar). This mechanism for vesicle formation is analogous to that for catanionic surfactant mixtures.[6]

To explain the effect of temperature, we postulate that the binding (adsorption) of counterions is a reversible process.[7,8] At low temperatures, the 5mS counterions will mostly remain bound to the aggregates. However, upon heating, a fraction of bound counterions will tend to desorb from the aggregates. This desorption will be promoted by the increase in solubility of 5mS in water with increasing temperature. As mentioned, 5mS has a limited solubility in water, but this value increases with temperature. Our measurements show that the solubility increases from 7.4 mM at 25°C to 18.9 mM at 85°C. Thus, 5mS has an increased affinity for water at higher temperatures, which could help explain its desorption from the micelle. The desorption will increase the effective headgroup area and thereby drive the system to aggregates of higher curvature. Such a mechanism can explain why we observe a transition from vesicles to wormlike micelles and thereby a viscosity increase.

As shown by Figure 3.10, we can view the concentration and temperature effects to be analogous. Thus, vesicles are formed when the effective 5mS concentration at the aggregate interface is high. This can be reached either by adding more 5mS to the solution or by lowering the temperature. Conversely, increasing the temperature reduces the effective 5mS concentration at the aggregate surface and induces micelles. This mechanism is similar to that invoked in previous studies of vesicle to micelle transitions induced by temperature.[7,8,31]

The above mechanism can also help explain the experimental trends in the transition temperature. For example, Figure 3.5 showed that the transition temperature increased with increasing [5mS]. This is because in samples with a higher [5mS], more of the [5mS] has to desorb before the transition point can be reached; this requires the sample to be heated to a higher temperature. Along these lines, preliminary experiments with different surfactant concentrations (data not shown) confirm that the [5mS]:[CTAB] ratio controls the onset of the vesicle to micelle phase transition.

3.5 CONCLUSIONS

In this study, we have shown that the aromatic derivative, 5-methyl salicylic acid (5mS) can induce the cationic surfactant, CTAB to form either wormlike micelles or unilamellar vesicles depending on the solution composition. Additionally, we have demonstrated that CTAB/5mS vesicles can be transformed into long, flexible "wormlike" micelles by heating the solution beyond a critical temperature. The vesicle to micelle transition causes the solutions to switch from low-viscosity, Newtonian fluids to

viscoelastic, shear-thinning fluids. The zero-shear viscosities of these fluids increase dramatically (by more than a factor of 1000) during this process. We used SANS to confirm the phase transition from vesicles to micelles, and our analysis of the data by the IFT method shows that there is a range of temperatures over which vesicles co-exist with the micelles. Finally, we have proposed a qualitative mechanism to account for the vesicle to micelle transition. This mechanism involves the desorption of bound aromatic counterions from the vesicle as temperature is increased.

Chapter 4. CONCLUSIONS AND FUTURE DIRECTIONS

4.1 CONCLUSIONS

In this work we have studied a new type of self-assembled fluid that exhibits an unusual temperature response. The system we have studied, consisting of mixtures of CTAB and 5mS, can spontaneously self assemble at low temperatures into a unilamellar vesicle phase over a range of concentrations. At elevated temperatures, the same solutions form elongated micellar chains. The transition between these two microstructures is perfectly reversible. Visual and turbidimetric observations allowed us to pinpoint the onset of the vesicle to micelle transition and we could tune this onset by varying the composition. The rheological data shows a sharp increase in viscosity (more than 1000-fold) with increasing temperature in these solutions.

Small angle neutron scattering (SANS) proved to be an invaluable tool in the characterization of the microstructures present in our systems. Without *a priori* information regarding the microstructure, we were able to model the SANS data using the Indirect Fourier Transform (IFT) methodology to elucidate the most probable structures present in the system. Using these methods, we have been able to show that the vesicle to micelle transition is a continuous, 2^{nd} order transition. Thus, at the onset of the transition, some of the vesicles begin to change into micelles while others remain unchanged. There is a co-existence of vesicles and micelles for a few degrees of temperature, until the entire population of vesicles is transformed into micelles.

Lastly, a mechanism for the vesicle to micelle transition has been proposed. This mechanism postulates a decrease in counter-ion binding to the interface of the aggregates with an increase in temperature. Our mechanism is in agreement with other work in this area and with some of our experimental studies with 5mS in aqueous solution.

4.2 FUTURE DIRECTIONS

This work provides a foundation for various directions in the future. We have shown that by varying the concentration of 5mS, the transition temperature can be tailored, as well as the magnitude of the viscosity increase. Similar experiments can also be done with varying the CTAB concentration. Further work can also focus on the effect of pH on the system, as the aromatic counter-ion is sensitive to slight changes in pH. Since this affects the solubility of the counter-ion, it is likely that changes in pH will affect how it will bind to the microstructures.

Further, since the transition can be tailored such that the vesicle to micelle transition occurs near room temperature, studies including a small amount of a photosensitive molecule can be carried out to explore the possibility of inducing a reversible transition from vesicles to micelles using light.[30] With the addition of a photoresponsive molecule, the packing parameter of the system can be altered by either a photoisomerization or photodimerization. This change in molecular geometry can force the formation of a different microstructure. Previous experiments on a light-induced vesicle to micelle transition required complex synthesis and purification of novel

surfactants.[30] The present system is much simpler for this purpose. Such studies are currently under way in the lab.

Lastly, for applications of the vesicles in drug delivery, it will be interesting to entrap the vesicles in a polymer hydrogel matrix. One could then heat the hydrogel lightly to induce breakage of vesicles into micelles. This would release the drug into the matrix of the gel. Similarly, one could use associating polymers to stabilize these vesicles in networks. Then, using only heat, these stabilized systems can be broken down releasing the trapped molecules. This release can be measured as a function of time and temperature. Such materials could serve as model systems for the controlled release of drugs or other molecules.

REFERENCES

[1] Evans, D. F.; Wennerstrom, H. *The Colloidal Domain: Where Physics, Chemistry, Biology, and Technology Meet*, Wiley-VCH: New York, 2001.

[2] Israelachvili, J. N. *Intermolecular and Surface Forces*, Academic Press: New York, 1992.

[3] Lasic, D. D. *Liposomes: From Physics to Applications*, Elsevier: Amsterdam, 1993.

[4] Cates, M. E.; Candau, S. J. "Statics and dynamics of worm-like surfactant micelles." *J. Phys.-Condens. Matter* **1990**, *2*, 6869-6892.

[5] Yang, J. "Viscoelastic wormlike micelles and their applications." *Curr. Opin. Colloid Interface Sci.* **2002**, *7*, 276-281.

[6] Kaler, E. W.; Murthy, A. K.; Rodriguez, B. E.; Zasadzinski, J. A. N. "Spontaneous vesicle formation in aqueous mixtures of single-tailed surfactants." *Science* **1989**, *245*, 1371-1374.

[7] Hassan, P. A.; Valaulikar, B. S.; Manohar, C.; Kern, F.; Bourdieu, L.; Candau, S. J. "Vesicle to micelle transition: Rheological investigations." *Langmuir* **1996**, *12*, 4350-4357.

[8] Buwalda, R. T.; Stuart, M. C. A.; Engberts, J. "Wormlike micellar and vesicular phases in aqueous solutions of single-tailed surfactants with aromatic counterions." *Langmuir* **2000**, *16*, 6780-6786.

[9] Larson, R. G. *The Structure and Rheology of Complex Fluids*, Oxford University Press: New York, 1998.

[10] Gravsholt, S. "Viscoelasticity in highly dilute aqueous-solutions of pure cationic detergents." *J. Colloid Interface Sci.* **1976**, *57*, 575-577.

[11] Imae, T.; Kamiya, R.; Ikeda, S. "Formation of spherical and rod-like micelles of cetyltrimethylammonium bromide in aqueous NaBr solutions." *J. Colloid Interface Sci.* **1985**, *108*, 215-225.

[12] Gamboa, C.; Sepulveda, L. "High viscosities of cationic and anionic micellar solutions in the presence of added salts." *J. Colloid Interface Sci.* **1986**, *113*, 566-576.

[13] Gamboa, C.; Rios, H.; Sepulveda, L. "Effect of the nature of counterions on the sphere-to-rod transition in cetyltrimethylammonium micelles." *J. Phys. Chem.* **1989**, *93*, 5540-5543.

[14] Rehage, H.; Hoffmann, H. “Viscoelastic surfactant solutions - model systems for rheological research.” *Mol. Phys.* **1991**, *74*, 933-973.

[15] Hoffmann, H. "Viscoelastic surfactant solutions." in *Structure and Flow in Surfactant Solutions*; Herb, C. A., Prud'homme, R. K., Eds.; American Chemical Society: Washington, DC, 1994; pp 2-31.

[16] Candau, S. J.; Hirsch, E.; Zana, R.; Adam, M. “Network properties of semidilute aqueous KBr solutions of cetyltrimethylammonium bromide.” *J. Colloid Interface Sci.* **1988**, *122*, 430-440.

[17] Imae, T.; Ikeda, S. “Sphere rod transition of micelles of tetradecyl trimethyl-ammonium halides in aqueous sodium-halide solutions and flexibility and entanglement of long rodlike micelles.” *J. Phys. Chem.* **1986**, *90*, 5216-5223.

[18] Kern, F.; Lemarechal, P.; Candau, S. J.; Cates, M. E. “Rheological properties of semidilute and concentrated aqueous solutions of cetyltrimethylammonium bromide in the presence of potassium bromide.” *Langmuir* **1992**, *8*, 437-440.

[19] Lin, Z.; Cai, J. J.; Scriven, L. E.; Davis, H. T. “Spherical-to-wormlike micelle transition in CTAB solutions.” *J. Phys. Chem.* **1994**, *98*, 5984-5993.

[20] Appell, J.; Porte, G. “Polymer-like behavior of giant micelles.” *Europhys. Lett.* **1990**, *12*, 185-190.

[21] Manohar, C.; Rao, U. R. K.; Valaulikar, B. S.; Iyer, R. M. “On the origin of viscoelasticity in micellar solutions of cetyltrimethylammonium bromide and sodium salicylate.” *J. Chem. Soc. - Chem. Commun.* **1986**, 379-381.

[22] Olsson, U.; Soderman, O.; Guering, P. “Characterization of micellar aggregates in viscoelastic surfactant solutions - a nuclear-magnetic-resonance and light-scattering study.” *J. Phys. Chem.* **1986**, *90*, 5223-5232.

[23] Shikata, T.; Hirata, H.; Kotaka, T. “Micelle formation of detergent molecules in aqueous-media. 3. Viscoelastic properties of aqueous cetyltrimethylammonium bromide salicylic-acid solutions.” *Langmuir* **1989**, *5*, 398-405.

[24] Macosko, C. W. *Rheology: Principles, Measurements and Applications*, VCH Publishers: New York, 1994.

[25] Zemb, T.; Lindner, P., Eds.; *Neutron, X-Ray and Light Scattering: Introduction to an Investigative Tool for Colloidal and Polymeric Systems*; Elsevier: Amsterdam, 1991.

[26] Glatter, O. “New method for evaluation of small-angle scattering data.” *J. Appl. Crystallogr.* **1977**, *10*, 415-421.

[27] Glatter, O.; Fritz, G.; Lindner, H.; Brunner-Popela, J.; Mittelbach, R.; Strey, R.; Egelhaaf, S. U. “Nonionic micelles near the critical point: Micellar growth and attractive interaction.” *Langmuir* **2000**, *16*, 8692-8701.

[28] Zheng, Y.; Lin, Z.; Zakin, J. L.; Talmon, Y.; Davis, H. T.; Scriven, L. E. “Cryo-TEM imaging the flow-induced transition from vesicles to threadlike micelles.” *J. Phys. Chem. B* **2000**, *104*, 5263-5271.

[29] Hassan, P. A.; Fritz, G.; Kaler, E. W. “Small angle neutron scattering study of sodium dodecyl sulfate micellar growth driven by addition of a hydrotropic salt.” *J. Colloid Interface Sci.* **2003**, *257*, 154-162.

[30] Hubbard, F. P.; Santonicola, G.; Kaler, E. W.; Abbott, N. L. “Small-angle neutron scattering from mixtures of sodium dodecyl sulfate and a cationic, bolaform surfactant containing azobenzene.” *Langmuir* **2005**, *21*, 6131-6136.

[31] Miguel, M. D.; Eidelman, O.; Ollivon, M.; Walter, A. “Temperature-dependence of the vesicle-micelle transition of egg phosphatidylcholine and octyl glucoside.” *Biochemistry* **1989**, *28*, 8921-8928.

[32] Egelhaaf, S. U.; Schurtenberger, P. “Micelle-to-vesicle transition: A time-resolved structural study.” *Phys. Rev. Lett.* **1999**, *82*, 2804-2807.

[33] Lesieur, P.; Kiselev, M. A.; Barsukov, L. I.; Lombardo, D. “Temperature-induced micelle to vesicle transition: Kinetic effects in the DMPC/NaC system.” *J. Appl. Crystallogr.* **2000**, *33*, 623-627.

[34] Xia, Y.; Goldmints, I.; Johnson, P. W.; Hatton, T. A.; Bose, A. “Temporal evolution of microstructures in aqueous CTAB/SOS and CTAB/HDBS solutions.” *Langmuir* **2002**, *18*, 3822-3828.

[35] Yin, H. Q.; Zhou, Z. K.; Huang, J. B.; Zheng, R.; Zhang, Y. Y. “Temperature-induced micelle to vesicle transition in the sodium dodecyl sulfate / dodecyl triethylammonium bromide system.” *Angew. Chem.-Int. Edit.* **2003**, *42*, 2188-2191.